CARBOHYDRATE POLYMERS

Volume 102, 15 February 2014, Pages 821–829

http://dx.doi.org/10.1016/j.carbpol.2013.10.083

http://www.sciencedirect.com/science/article/pii/S0144861713011120

THERMOPLASTIC STARCH/WOOD COMPOSITES: INTERFACIAL INTERACTIONS AND FUNCTIONAL PROPERTIES

Péter Müller[1], Károly Renner[1,2], János Móczó[1,2*], Erika Fekete[1,2], Béla Pukánszky[1,2]

[1]Laboratory of Plastics and Rubber Technology, Department of Physical Chemistry and Materials Science, Budapest University of Technology and Economics, H-1521 Budapest, P.O. Box 91, Hungary

[2]Institute of Materials and Environmental Chemistry, Research Centre for Natural Sciences, Hungarian Academy of Sciences, H-1525 Budapest, P.O. Box 17, Hungary

*Corresponding author: Phone: +36-1-463-3477, Fax: +36-1-463-3474, Email: jmoczo@mail.bme.hu

ABSTRACT

Thermoplastic starch (TPS)/wood composites were prepared from starch plasticized with 36 wt% glycerol. The components were homogenized by dry-blending, extruded and injection molded to tensile bars. Tensile properties, structure, deformation, water adsorption and shrinkage were determined as a function of wood content, which changed between 0 and 40 vol% in 7 steps. The modification of TPS with wood particles improves several properties considerably. Stiffness and strength increases, and the effect is stronger for fibers with larger aspect ratio. Wood fibers reinforce TPS considerably due to poor matrix properties and strong interfacial interactions, the latter resulting in the decreased mobility of starch molecules and in the fracture of large wood particles during deformation. Strong interfacial adhesion leads to smaller water absorption than predicted from additivity, but water uptake remains relatively large even in the presence of wood particles. The shrinkage of injection molded TPS parts is very large, around 10 %, and dimensional changes occur on a very long timescale of several hundred hours. Shrinkage decreases to a low level already at 15-20 vol% wood content rendering the composites good dimensional stability.

KEYWORDS: TPS/wood composites, particle characteristics, interfacial adhesion, water absorption, shrinkage

1. INTRODUCTION

The constant threat of depleting fossil fuel sources and the increasing environmental awareness of the public resulted in increasing interest in natural polymers in all fields of life (Markarian 2008). Cellulose, lignin and starch are renewable materials produced in very large quantities each year. The use of natural-based raw materials or additives in plas-

tics has become industrial practice recently and as a consequence, the interest of the scientific community increased as well. Cellulose and wood are used as reinforcement, lignin to produce various chemicals, while under some conditions starch is applied as a thermoplastic polymer. Starch itself cannot be processed with traditional thermoplastic processing technologies because of the large size and stiffness of the molecules, and the resulting high glass transition temperature. Because of strong hydrogen bonds developing among the molecules, neat starch cannot be melted and processed without further treatment (Jang & Pyun 1996; Swanson et al. 1993). Chemical modification and plasticization partially resolves these problems and plasticized starch can be processed by extrusion, injection molding or other processing methods. Besides the advantages (processability, flexibility, biodegradability, etc.) of plasticized starch, it also has disadvantages like poor mechanical properties, water sensitivity, poor dimensional instability, etc. In order to overcome these drawbacks thermoplastic starch (TPS) is often modified by blending with other polymers (Cerclé et al. 2013; Landreau et al. 2009; Shirai et al. 2013; Shujun et al. 2005), the addition of fillers or reinforcements (Castillo et al. 2013; de Carvalho et al. 2001; Kuciel et al. 2012; Ma et al. 2005) or the preparation of nanocomposites (Bagdi et al. 2006; Castillo et al. 2013; Huang et al. 2004). In order to maintain one of the most important advantages of starch, i.e. biodegradability, it is modified mostly with aliphatic polyesters and natural fibers (Avérous et al. 2001; Benezet et al. 2012; Chakraborty et al. 2007; Huang et al. 2004; Shirai et al. 2013; Sreekumar et al. 2010; Torres et al. 2007).

A considerable number of papers deal with the effect of natural fibers on the properties of thermoplastic starch. Most of them study the influence of fiber type and amount usually determining properties at one or two fiber contents. All kinds of fibers have been used as reinforcement in TPS including various forms of cellulose (Avérous et al. 2001 (natural cellulose fibers from leafwood); Ayadi & Dole 2011 (natural cellulose fibers from

leafwood); Benezet et al. 2012 (wheat straw fibers, hemp fibers, cotton linter fibers); Curvelo et al. 2001 (bleach pulp fiber); Ma et al. 2005 (micro winceyette fibers); Martins et al. 2009 (bacterial cellulose and vegetable cellulose fibers); Muller et al. 2009; Soykeabkaew et al. 2012 (bacterial cellulose); Soykeabkaew et al. 2004 (jute and flax fibers); Sreekala et al. 2008), jute (Soykeabkaew et al. 2012; Torres et al. 2007; Wollerdorfer & Bader 1998), sisal (Girones et al. 2012; Sreekumar et al. 2010a; Sreekumar et al. 2010b; Torres et al. 2007; Wang et al. 2012), wheat straw (Benezet et al. 2012), hemp (Benezet et al. 2012; Girones et al. 2012; Kunanopparat et al. 2008; Ochi 2006), cotton (Benezet et al. 2012; Moriana et al. 2010; Prachayawarakorn et al. 2010), flax (Saiah et al. 2009; Soykeabkaew et al. 2004), ramie (Lu et al. 2006; Sreekala et al. 2008), etc. Somewhat less papers deal with TPS/wood composites (Abbott et al. 2012; Agnantopoulou et al. 2012; Avérous & Boquillon 2004; Chakraborty et al. 2007; Kuciel et al. 2012; Kuciel & Liber-Knec 2009), although wood is cheaper and simpler to handle during processing. Some of the papers cited investigates the effect of fiber characteristics on mechanical properties and conclude that stiffness and strength increase both with increasing fiber length and content. (Avérous et al. 2001). Others, but much fewer in number, also mention interfacial interactions and based mostly on SEM micrographs (Avérous et al. 2001; Lu et al. 2006; Prachayawarakorn et al. 2011), the shift of absorption bands in FTIR (Prachayawarakorn et al. 2011), and changing glass transition temperature deduce that interfacial adhesion is strong between natural fibers and starch (Avérous & Boquillon 2004; Avérous et al. 2001; Curvelo et al. 2001; Martins et al. 2009; Soykeabkaew et al. 2012). Limited number of attempts exist which estimate interfacial adhesion quantitatively (Avérous & Boquillon 2004).

Since water sensitivity is a drawback of starch composites, its change with fiber modification is studied relatively often and the results generally indicate that water absorp-

tion decreases with increasing fiber content (Ayadi & Dole 2011; Curvelo et al. 2001; Lu et al. 2006; Ma et al. 2005; Soykeabkaew et al. 2012). This change is explained with the smaller water uptake of the fibers compared to that of starch. Attempts to determine the dimensional stability of starch/fiber composites are much less frequent, although shrinkage might be considerable hindering application in some areas. Existing papers indicate that shrinkage decreases with increasing fiber content, i.e. modification is beneficial from this aspect as well (Avérous et al. 2001).

The study of existing literature indicated that considering their practical relevance relatively small number of papers have been published on TPS/wood composites (Abbott et al. 2012; Agnantopoulou et al. 2012; Avérous & Boquillon 2004; Chakraborty et al. 2007; Kuciel et al. 2012; Kuciel & Liber-Knec 2009). Even less report systematic experiments carried out as a function of fiber content in a wide composition range (Abbott et al. 2012; Agnantopoulou et al. 2012; Avérous & Boquillon 2004). As a consequence, the goal of our work was to prepare TPS/wood composites with wood fillers of different particle characteristics, determine their reinforcing effect and influence on properties in a wide composition range. Considerable attention is paid to interfacial interactions, and reinforcement as well as interfacial adhesion are estimated quantitatively in comparison with commodity polymer/wood composites. The effect of wood characteristics and content on water absorption and shrinkage were studied and are discussed in detail.

2. EXPERIMENTAL

The corn starch used in the experiments was supplied by Hungrana Ltd. Hungary and its water content was 12 %. Glycerol with 0.5 % water content was obtained from Molar Chemicals Ltd. Hungary and it was used without further purification or drying. Three different wood fibers were used as reinforcement, all three obtained from Rettenmaier and

Söhne GmbH, Germany. The particle characteristics of the fibers are listed in Table 1. Since in several of our previous projects aspect ratio turned out to be one of the most important characteristics of wood fibers (Renner et al. 2010a; Renner et al. 2009), we included it into the abbreviation of the samples used. Accordingly, WP126 indicates a wood fiber with an aspect ratio of 12.6. Composites were prepared with 5, 10, 15, 20, 30 and 40 vol% wood content.

Both corn starch and the fibers were dried in an oven before composite preparation (100°C for 24 hours and 105 °C for 4 hours, respectively). Thermoplastic starch containing 36 wt% glycerol was prepared by dry-blending in a Henschel FM/A10 high speed mixer at 2000 rpm. The wood fibers were introduced into the mixer at the end of the plasticization process. TPS was produced by processing the dry-blend on a Rheomex 3/4" single screw extruder attached to a Haake Rheocord EU 10 V driving unit at 140-150-160 °C barrel and 170 °C die temperatures, and 60 rpm screw speed. TPS was injection molded into standard ISO 527-1A tensile bars using a Battenfeld BA 200 CD hydraulic machine at 140-160-170 °C barrel, 180 °C nozzle and 40 °C mold temperatures, 140 bar injection pressure, 54 mm/s injection rate, and 35 s cooling time.

The mechanical properties of the specimens were characterized by tensile testing using an Instron 5566 universal testing machine at 5 mm/min cross-head speed and 115 mm gauge length at 23 °C and 50 % RH. Micromechanical deformations during tensile testing were followed by recording acoustic emission signals with a Sensophone AED 40/4 apparatus with 20 db threshold. The particle characteristics of the fibers and composite structure were characterized by polarized optical (POM) and scanning electron microscopy (SEM). POM micrographs were recorded on cryo-cut slices of 10 μm thickness with cross polarizers using a Leitz EM FC7 microscope. SEM micrographs (Jeol JSM-6380) were taken from the fracture surface of composite samples created during tensile

testing. The crystalline structure of the TPS matrix, the wood fibers and the composites was characterized by X-ray diffraction using a Phillips PW 1830/PW 1050 equipment with CuK_{α} radiation at 40 kV and 35 mA anode excitation. Glass transition temperature and other thermal transitions were determined with dynamic mechanical analysis using a Perkin Elmer Pyris Diamond DMA apparatus in single cantilever mode with constant amplitude (10 μm) and frequency (1 Hz) in the temperature range between -100 and 80 °C with a heating rate of 2 °C/min. Water absorption was determined at 23 °C and 52 % relative humidity by the measurement of the weight increase of the specimens. The desired relative humidity was achieved with saturated solution of $Mg(NO_3)_2$. Shrinkage was followed by the measurement of the length of the specimens as a function of time. The specimens were kept in a desiccator over silica gel to avoid the complicating influence of water absorption.

3. RESULTS AND DISCUSSION

The results are presented in several sections. Mechanical properties and structure are described first and then the reinforcing effect of the fiber is discussed in the next section. Special attention is paid to interfacial interactions, and the effect of wood reinforcement on functional properties is discussed in the final section of the paper.

3.1. Structure and mechanical properties

Aggregation, attrition and orientation of anisotropic particles are the most important structure related phenomena in particulate filled and fiber reinforced composites. Previous studies on wood reinforced composites have shown that aggregation rarely occurs, but fibers might touch each other purely from geometric reasons (Dányádi et al. 2010; Dányádi et al. 2007; Renner et al. 2010a; Renner et al. 2009). Long fibers may even form a loose network (Faludi et al. 2013). SEM micrographs taken from the fracture sur-

face of two composites is shown in **Figs. 1a and 1b**. A single large particle embedded into the matrix is seen in **Fig. 1a** presenting the micrograph recorded on a TPS/W68 composite containing 10 vol% wood. In **Fig. 1b** several broken fibers appear on the surface of a TPS/W126 composite of the same composition and the micrograph clearly indicates the good dispersion of the particles. One must be aware of the fact that SEM micrographs can always be debated and they can be used only as supplementary evidence to support conclusions from other results. Nevertheless, they can demonstrate the fracture of the fibers quite well as shown by **Fig. 1b**. They are completely inadequate to demonstrate homogeneity and the quality of dispersion cannot be judged reliably based on them. On the other hand, POM micrographs taken at smaller magnification offer a clear picture of structure (**Figs. 1c and 1d**). Such a micrograph recorded on a TPS/W126 composite at 5 vol% wood content shows the homogeneous distribution of the fibers in the TPS matrix (**Fig. 1c**). At 40 vol% wood content the fibers touch each other (**Fig. 1d**) as shown earlier (Faludi et al. 2013), but real aggregates do not form even at this fiber loading. Nevertheless, the physical contact of the fibers probably influences mechanical properties to some extent. Microscopy clearly proves that the distribution of wood particles is homogeneous at small, but physical contacts form among them at large fiber contents.

Stiffness is used the most frequently to estimate the effect of fillers and fibers on the properties of composites. The modulus of our TPS/wood composites is plotted against fiber content in **Fig. 2a**. According to the figure stiffness increases from around 0.35 GPa up to approximately 4.5 GPa, i.e. modification with wood results in very strong reinforcement. The initial steep increase slows down at larger fiber contents indicating some structural effect, probably the mere physical contact of the particles discussed above (Dányádi et al. 2007; Renner et al. 2010a; Renner et al. 2009) or the formation of a network in the case of fibers with large aspect ratio (Faludi et al. 2013b). The composition

dependence of mechanical properties strongly supports this explanation since the largest deviation from the tendency observed at large fiber content occurs for the small (W35) and the long (W126) fibers (see **Table 1**). This latter has larger reinforcing effect at small fiber contents than the other two wood flours (W35, W68).

The tensile strength of composites containing the three wood fibers is plotted against wood content in **Fig. 2b**. The same conclusions can be drawn here as from the composition dependence of modulus. Strength increases at least as strongly as stiffness and the different fibers influence also this property dissimilarly. Small (W35) and long particles (W126) reinforce TPS more than the third wood flour (W68), but structural effects are also stronger in the former two cases. Deformability, i.e. the elongation-at-break of the specimens decreases drastically with increasing wood content (**Fig. 2c**), but such an effect is usually expected both in particulate filled and fiber reinforced composites. The effect of the three fibers is very similar; specific surface area seems to influence deformability, but differences are quite small. We can conclude from these results that wood reinforcement is beneficial if stiffness and strength are the targeted properties, considerable reinforcement occurs, but its extent is difficult to judge from the qualitative evaluation of the results.

3.2. Reinforcement

Reinforcement, i.e. the load-bearing capacity of the second component, can be estimated quantitatively by the use of the simple model developed earlier to describe the composition dependence of tensile yield stress (Turcsányi et al. 1988), tensile strength (Pukánszky 1990) or fracture resistance (Pukánszky & Maurer 1995) of particulate filled polymers. The model takes the following form for tensile strength

$$\sigma_T = \sigma_{T0}\,\lambda^n\,\frac{1-\varphi}{1+2.5\,\varphi}\exp(B\,\varphi) \qquad (1)$$

where σ_T and σ_{T0} are the true tensile strength ($\sigma_T = \sigma\lambda$ and $\lambda = L/L_0$) of the composite and the matrix, respectively, n is a parameter taking into account strain hardening, φ is the volume fraction of the fiber and B is related to its relative load-bearing capacity, i.e. to the extent of reinforcement, which, among other factors, depends also on interfacial interaction. If we transform Eq. 1 into a linear form and plot the natural logarithm of reduced tensile strength against fiber content, we obtain a linear correlation (**Fig. 3a**), the slope of which is proportional to the load-bearing capacity of the reinforcement and under certain conditions to the strength of interaction. The correlations are linear at small fiber loadings indeed, but deviations are observed at large wood contents. Such deviations usually indicate structural effects, i.e. they confirm our tentative explanation presented in the previous section. The slope of the straight lines is parameter *B*, which expresses the load-bearing capacity of the second component, i.e. reinforcement. The value of *B* ranges from 9.4 to 12.6 for the three wood fibers used, and they are very large compared to usual particulate filled commodity polymers; *B* is often smaller than 1 for PP/$CaCO_3$ composites, for example (Kiss et al. 2007; Pukánszky 1990).

The reinforcing effect of a filler or fiber depends on interfacial interactions, but also on the properties of the matrix (σ_0), which plays an important role in the actual value of *B*. This role can be seen even better if we plot *B* values as a function of the natural logarithm of reciprocal matrix strength, i.e. $\ln(1/\sigma_0)$ (see Pukánszky, 1990). The correlation is presented for various thermoplastic wood composites in **Fig. 3b**. We can see that the inherent property of the matrix dominates in the determination of the extent of reinforcement. However, reinforcement depends also on interfacial adhesion, thus we need further study and analysis to define its strength.

3.3. Interfacial adhesion

As described in the introductory part, several approaches are used to estimate the strength of interfacial interactions in TPS/natural fiber composites. FTIR and the determination of the glass transition temperature were mentioned as specific examples. The temperature dependence of the loss modulus of TPS and that of the composites containing the three wood reinforcements at 30 vol% is plotted in **Fig. 4**. Both TPS and the composites exhibit two transitions, one at low temperature which can be assigned to the relaxation of smaller structural units and which is related to the amount of glycerol (Avérous & Pollet 2012; Forssell et al. 1997), while the second above room temperature which is identified as the glass transition temperature of TPS. Reinforcement with wood results in considerable increase of this latter indicating large decrease in the mobility of starch molecules. This is rather surprising, since very small changes can be seen in the T_g of particulate filled polymers and only at large contact surfaces (Bleach et al. 2002; Mortezaei et al. 2010). The probable reasons for the large effect are strong hydrogen bonds and the stiffness of starch molecules; a few secondary bonds are sufficient to decrease mobility. Even the presence and competitive interaction of the small glycerol molecules do not influence this effect. Wood properties do not seem to play a role here, but we must call the attention here to the fact that the specific surface area of the three fillers is very similar. We can conclude that strong interactions develop between TPS and wood at the segmental and molecular level, but we do not know much about macroscopic interfaces.

Various deformation processes may take place around the inclusions in composites. Besides debonding, i.e. the separation of the interface between the matrix and the reinforcement, several other processes including matrix yielding, the pull-out or fracture of the fibers, cavitation, etc. may also take place during the deformation of the composites (Dányádi et al. 2007; Faludi et al. 2013a; Imre et al. 2012; Renner et al. 2007; Renner et

al. 2010b). Some of these are burst-like processes emitting elastic waves, which can be picked up by appropriate sensors. The result of such an acoustic emission measurement is presented in **Fig. 5a**. The small circles are individual acoustic events (signals); one of the continuous lines shows the cumulative number of events (right axis), while the other is the stress vs. elongation trace (left axis) shown as reference. We can see that no acoustic activity can be detected below certain deformation or stress, and a characteristic stress (σ_{AE}) can be determined in the way indicated in **Fig. 5a**. This stress is related to the initiation of the dominating micromechanical deformation process taking place around wood particles upon deformation. The composition dependence of this characteristic stress is plotted against wood content in **Fig. 5b**. We can see differences in the effect of the three fibers; the longest and largest fibers initiate the process at larger, while the small particles at smaller stress. We cannot identify the dominating deformation process either from the value of the characteristic stress or the shape of the cumulative number of signal trace; it can be debonding or the fracture of the wood particles, as shown earlier (Dányádi et al. 2007; Renner et al. 2010a; Renner et al. 2009).

If debonding is the dominating process, interfacial adhesion can be estimated quantitatively with the help of a model developed earlier (Pukánszky & Vörös 1993). According to the model debonding stress can be expressed as

$$\sigma^D = -C_1 \sigma^T + C_2 \left(\frac{E F_a}{R} \right)^{1/2} \qquad (2)$$

where σ^D and σ^T are debonding and thermal stresses, respectively, E the Young's modulus of the matrix, F_a the strength of interfacial adhesion, which is equal to the reversible work of adhesion, if adhesion is created by secondary forces, R the radius of the particles, while C_1 and C_2 are geometric constants related to the debonding process. The parameters of the equation were calculated from measurements done on polymer/filler pairs with known

characteristics (E, R, F_a). If we know the stiffness of the matrix and the size of the particles, which we usually do, we can calculate the strength of adhesion (F_a) (Renner et al. 2010c). In our case we can assume that $\sigma^D = \sigma_{AE}$ and calculate F_a from **Eq. 2**. The results are listed in **Table 2** for the three set of composites. Polypropylene (PP) reinforced with one of the fillers (W35) is used as reference. PP is a commodity polymer used in large quantities also as the matrix of wood composites. Moreover, interfacial adhesion can be changed considerably by coupling, thus the adhesion values determined at poor and good adhesion can serve well as reference. In the absence of coupling interaction is poor in PP, while covalent bonds are assumed to form when a functionalized coupling agent (MAPP) is used. We can see one order of magnitude difference in the strength of adhesion in the two cases. The adhesion calculated in the TPS composite containing the small particles (W35) is similar that that determined in PP at good adhesion, but considerably larger values are obtained for the other two fibers indicating very good adhesion. Since parameter B appearing in **Eq. 1** is also related to interfacial adhesion, we can use it also for the estimation of the strength of interaction, but we must compensate for the effect of changing matrix property. We did that by multiplying B by $\ln(1/\sigma_0)$ and the results are also listed in **Table 2.** They convey practically the same message as F_a, i.e. interfacial adhesion is very strong in TPS/wood composites. Even if not debonding, but some other mechanism dominates in TPS composites, it is certain that strong interfacial interaction develops between the components considerably influencing properties.

We could not define the dominating micromechanical deformation process taking place during the deformation of TPS/wood composites from the composition dependence of properties or from acoustic emission measurements. We assumed that SEM micrographs taken from fracture surfaces created during tensile testing would offer further information about interfacial adhesion and processes occurring around the particles. Two

micrographs taken from composites containing 10 vol% fibers were presented in **Figs. 1a and b** in a previous section. The fracture surface of the TPS/W68 composite presented in **Fig. 1a** shows a very large broken particle which is firmly embedded in the matrix. A larger number of broken fibers can be observed on the surface of the TPS/W126 composite. Most of the fibers fracture perpendicularly to their axis, which occurs only at very strong interactions. In spite of all uncertainties of the method, the SEM study obviously supports our conclusion that interaction is strong in the TPS/wood composites studied and not debonding, but fiber fracture is the dominating process. Apart from the firm embedding of the particles into the TPS matrix, very few characteristic features can be seen on the fracture surface of TPS/W35 composites (not shown).

3.4. Functional properties

In order to fulfill their function, products prepared from TPS composites must satisfy certain conditions. The adsorption of excessive water modifies properties, stiffness and strength decrease or the part can fail completely. Similarly, shrinkage may result in unacceptable dimensional changes. Earlier studies showed that the reinforcement of TPS with natural fibers decreases its water uptake, i.e. results in the improvement of this characteristic (Ayadi & Dole 2011; Curvelo et al. 2001; Lu et al. 2006; Ma et al. 2005; Soykeabkaew et al. 2012). Equilibrium water absorption was determined from adsorption isotherms by fitting the following form of Fick's law to the experimental results

$$M_t = M_\infty \left(1 - \frac{8}{\pi^2}\left(\exp(-a\,t) + \frac{1}{9}\exp(-9\,a\,t) + \frac{1}{25}\exp(-25\,a\,t)\right)\right) \qquad (5)$$

where M_t is time dependent weight increase, M_∞ the final (equilibrium) water uptake reached after infinite time, t the time of adsorption and a a constant characterizing the overall rate of water adsorption. The equilibrium water uptake of the composites is plotted

in **Fig. 6** showing that water absorption decreases with wood content, as reported in the literature, and the effect of the three wood fibers is very similar. The broken line in **Fig. 6** indicates additivity, i.e. the value of water uptake calculated from that of TPS and wood for each composition. We can see that the actual water absorption of the composites is smaller than the additive value. A probable explanation might be the strong interaction between the components discussed in the previous section. We must call the attention here to the fact though, that water absorption is rather large even at 40 vol% wood content, i.e. it might hinder the application of these materials in certain fields.

The shrinkage of TPS is another important factor which may limit its application. **Fig. 7** shows the photo of injection molded TPS/W68 composite tensile bars with different fiber contents taken 345 days after production. A HDPE bar is used as reference. HDPE is a crystalline polymer with a relatively large shrinkage in engineering practice. Compared to commodity and especially to engineering thermoplastics the shrinkage of TPS is extremely strong and some warpage also occurs. Such shrinkage obviously cannot be tolerated in certain applications. We recorded XRD traces on the bars as a function of time to check if the slow crystallization of TPS results in the considerable shrinkage. We did not found any changes in crystalline structure and concluded that the reason of these large dimensional changes is the limited flexibility of the starch molecules and their long relaxation times. Injection molding results in non-equilibrium structure and the presence of the plasticizer allows relaxation, but only on a very long time scale. The time dependence of shrinkage is shown in **Fig. 8a** for the composites containing the large aspect ratio fibers (W126). Shrinkage increases with time according to a saturation function on a very long timescale. Shrinkage is very large for TPS, but the presence of already 5 vol% fiber decreases shrinkage considerably, while above 10 vol% shrinkage can be practically neglected, at least compared to that of neat TPS. We should like to call the attention here to the

long time scale of the experiment. The effect of wood content on the final, equilibrium shrinkage can be seen much better in **Fig. 8b** together with the effect of fiber characteristics. Shrinkage decreases very fast with increasing wood content and reaches very small values already at 15 vol% wood content. In accordance with literature data, fibers with larger aspect ratio hinder shrinkage in a larger extent than short particles. Obviously, wood reinforcement has very advantageous effect on the shrinkage of TPS and it may extend the application area for these materials considerably.

4. CONCLUSIONS

The modification of TPS with wood particles improves several properties considerably. Stiffness and strength increases, and the effect is stronger for fibers with larger aspect ratio. Wood fibers reinforce TPS considerably due to poor matrix properties and strong interfacial interactions, the latter resulting in the decreased mobility of starch molecules and in the fracture of large wood particles during deformation. Strong interfacial adhesion leads to smaller water absorption than predicted from additivity, but water uptake remains relatively large even in the presence of wood particles. The shrinkage of injection molded TPS parts is very large, around 10 %, and dimensional changes occur on a very long timescale of several hundred hours. Shrinkage decreases considerably to a low level already at 15-20 vol% wood content rendering the composites good dimensional stability. Wood reinforcement of TPS is generally advantageous for most application areas.

5. ACKNOWLEDGEMENTS

The authors are indebted to László Sinka for his help in composite production, specimen preparation and some measurements. The financial support of the National Scientific Research Fund of Hungary (OTKA Grant No. K 101124) to the research on hetero-

geneous polymer systems is appreciated very much.

6. REFERENCES

Abbott, A. P., Palazuela Conde, J., Davis, S. J., & Wise, W. R. (2012) Starch as a replacement for urea-formaldehyde in medium density fibreboard. *Green Chemistry 14*, 3067-3070.

Agnantopoulou, E., Tserki, V., Marras, S., Philippou, J., & Panayiotou, C. (2012) Development of biodegradable composites based on wood waste flour and thermoplastic starch. *Journal of Applied Polymer Science 126*, E273-E281.

Avérous, L., & Boquillon, N. (2004) Biocomposites based on plasticized starch: thermal and mechanical behaviours. *Carbohydrate Polymers 56*, 111-122.

Avérous, L., Fringant, C., & Moro, L. (2001) Plasticized starch-cellulose interactions in polysaccharide composites. *Polymer 42*, 6565-6572.

Avérous, L., & Pollet, E. (2012) Biodegradable Polymers. In *Environmental Silicate Nano-Biocomposites SE - 2* (ed. L. Avérous & E. Pollet), pp. 13-39. London: Springer.

Ayadi, F., & Dole, P. (2011) Stoichiometric interpretation of thermoplastic starch water sorption and relation to mechanical behavior. *Carbohydrate Polymers 84*, 872-880.

Bagdi, K., Müller, P., & Pukánszky, B. (2006) Thermoplastic starch/layered silicate composites: structure, interaction, properties. *Composite Interfaces 13*, 1-17.

Benezet, J. C., Stanojlovic-Davidovic, A., Bergeret, A., Ferry, L., & Crespy, A. (2012) Mechanical and physical properties of expanded starch, reinforced by natural fibres. *Industrial Crops and Products 37*, 435-440.

Bleach, N. C., Nazhat, S. N., Tanner, K. E., Kellomäki, M., & Törmälä, P. (2002) Effect of filler content on mechanical and dynamic mechanical properties of particulate

biphasic calcium phosphate-polylactide composites. *Biomaterials 23*, 1579-1585.

Castillo, L., López, O., López, C., Zaritzky, N., García, M. A., Barbosa, S., & Villar, M. (2013) Thermoplastic starch films reinforced with talc nanoparticles. *Carbohydrate Polymers 95*, 664-674.

Cerclé, C., Sarazin, P., & Favis, B. D. (2013) High performance polyethylene/thermoplastic starch blends through controlled emulsification phenomena. *Carbohydrate Polymers 92*, 138-148.

Chakraborty, A., Sain, M., Kortschot, M., & Cutler, S. (2007) Dispersion of Wood Microfibers in a Matrix of Thermoplastic Starch and StarchPolylactic Acid Blend. *Journal of Biobased Materials and Bioenergy 1*, 71-77.

Curvelo, A. A. S., de Carvalho, A. J. F., & Agnelli, J. A. M. (2001) Thermoplastic starch-cellulosic fibers composites: preliminary results. *Carbohydrate Polymers 45*, 183-188.

Dányádi, L., Móczó, J., & Pukánszky, B. (2010) Effect of various surface modifications of wood flour on the properties of PP/wood composites. *Composites Part A-Applied Science and Manufacturing 41*, 199-206.

Dányádi, L., Renner, K., Móczó, J., & Pukánszky, B. (2007) Wood flour filled polypropylene composites: Interfacial adhesion and micromechanical deformations. *Polymer Engineering and Science 47*, 1246-1255.

de Carvalho, A. J. F., Curvelo, A. A. S., & Agnelli, J. A. M. (2001) A first insight on composites of thermoplastic starch and kaolin. *Carbohydrate Polymers 45*, 189-194.

Faludi, G., Dora, G., Renner, K., Móczó, J., & Pukánszky, B. (2013a) Biocomposite from polylactic acid and lignocellulosic fibers: Structure-property correlations. *Carbohydrate Polymers 92*, 1767-1775.

Faludi, G., Hári, J., Renner, K., Móczó, J., & Pukánszky, B. (2013b) Fiber association and network formation in PLA/lignocellulosic fiber composites. *Composites Science and Technology 77*, 67-73.

Forssell, P. M., Mikkilä, J. M., Moates, G. K., & Parker, R. (1997) Phase and glass transition behaviour of concentrated barley starch-glycerol-water mixtures, a model for thermoplastic starch. *Carbohydrate Polymers 34*, 275-282.

Girones, J., Lopez, J. P., Mutje, P., Carvalho, A. J. F., Curvelo, A. A. S., & Vilaseca, F. (2012) Natural fiber-reinforced thermoplastic starch composites obtained by melt processing. *Composites Science and Technology 72*, 858-863.

Huang, M.-F., Yu, J.-G., & Ma, X.-F. (2004) Studies on the properties of Montmorillonite-reinforced thermoplastic starch composites. *Polymer 45*, 7017-7023.

Imre, B., Keledi, G., Renner, K., Móczó, J., Murariu, M., Dubois, P., & Pukánszky, B. (2012) Adhesion and micromechanical deformation processes in PLA/$CaSO_4$ composites. *Carbohydrate Polymers 89*, 759-767.

Jang, J. K., & Pyun, Y. R. (1996) Effect of Moisture Content on the Melting of Wheat Starch. *Starch - Stärke 48*, 48-51.

Kiss, A., Fekete, E., & Pukánszky, B. (2007) Aggregation of $CaCO_3$ particles in PP composites: Effect of surface coating. *Composites Science and Technology 67*, 1574-1583.

Kuciel, S., Kúzniar, P., Mikula, J., & Liber-Knéc, A. (2012) Mineral Microparticles and Wood Flour as Fillers of Different Biocomposites. *Journal of Biobased Materials and Bioenergy 6*, 475-480.

Kuciel, S., & Liber-Knec, A. (2009) Biocomposites on the Base of Thermoplastic Starch Filled by Wood and Kenaf Fiber. *Journal of Biobased Materials and Bioenergy 3*,

269-274.

Kunanopparat, T., Menut, P., Morel, M. H., & Guilbert, S. (2008) Reinforcement of plasticized wheat gluten with natural fibers: From mechanical improvement to deplasticizing effect. *Composites Part A-Applied Science and Manufacturing 39,* 777-785.

Landreau, E., Tighzert, L., Bliard, C., Berzin, F., & Lacoste, C. (2009) Morphologies and properties of plasticized starch/polyamide compatibilized blends. *European Polymer Journal 45,* 2609-2618.

Lu, Y. S., Weng, L. H., & Cao, X. D. (2006) Morphological, thermal and mechanical properties of ramie crystallites - reinforced plasticized starch biocomposites. *Carbohydrate Polymers 63,* 198-204.

Ma, X. F., Yu, J. G., & Kennedy, J. F. (2005) Studies on the properties of natural fibers-reinforced thermoplastic starch composites. *Carbohydrate Polymers 62,* 19-24.

Markarian, J. (2008) Biopolymers present new market opportunities for additives in packaging. *Plastics, Additives and Compounding 10,* 22-25.

Martins, I. M. G., Magina, S. P., Oliveira, L., Freire, C. S. R., Silvestre, A. J. D., Neto, C. P., & Gandini, A. (2009) New biocomposites based on thermoplastic starch and bacterial cellulose. *Composites Science and Technology 69,* 2163-2168.

Moriana, R., Karlsson, S., & Ribes-Greus, A. (2010) Assessing the Influence of Cotton Fibers on the Degradation in Soil of a Thermoplastic Starch-Based Biopolymer. *Polymer Composites 31,* 2102-2111.

Mortezaei, M., Famili, M. H. N., & Kokabi, M. (2010) Influence of the particle size on the viscoelastic glass transition of silica-filled polystyrene. *Journal of Applied Polymer Science 115,* 969-975.

Muller, C. M. O., Laurindo, J. B., & Yamashita, F. (2009) Effect of cellulose fibers on the

crystallinity and mechanical properties of starch-based films at different relative humidity values. *Carbohydrate Polymers 77*, 293-299.

Ochi, S. (2006) Development of high strength biodegradable composites using Manila hemp fiber and starch-based biodegradable resin. *Composites Part A-Applied Science and Manufacturing 37*, 1879-1883.

Prachayawarakorn, J., Ruttanabus, P., & Boonsom, P. (2011) Effect of Cotton Fiber Contents and Lengths on Properties of Thermoplastic Starch Composites Prepared from Rice and Waxy Rice Starches. *Journal of Polymers and the Environment 19*, 274-282.

Prachayawarakorn, J., Sangnitidej, P., & Boonpasith, P. (2010) Properties of thermoplastic rice starch composites reinforced by cotton or low-density polyethylene. *Carbohydrate Polymers 81*, 425-433.

Pukánszky, B. (1990) Influence of Interface Interaction on the Ultimate Tensile Properties of Polymer Composites. *Composites 21*, 255-262.

Pukánszky, B., & Maurer, F. H. J. (1995) Composition Dependence of the Fracture-Toughness of Heterogeneous Polymer Systems. *Polymer 36*, 1617-1625.

Pukánszky, B., & Vörös, G. (1993) Mechanism of interfacial interactions in particulate filled composites. *Composite Interfaces 1*, 411-427.

Renner, K., Henning, S., Móczó, J., Yang, M. S., Choi, H. J., & Pukánszky, B. (2007) Micromechanical deformation processes in PA/layered silicate nanocomposites: Correlation of structure and properties. *Polymer Engineering and Science 47*, 1235-1245.

Renner, K., Kenyó, C., Móczó, J., & Pukánszky, B. (2010a) Micromechanical deformation processes in PP/wood composites: Particle characteristics, adhesion, mechanisms. *Composites Part A-Applied Science and Manufacturing 41*, 1653-1661.

Renner, K., Móczó, J., & Pukánszky, B. (2009) Deformation and failure of PP composites reinforced with lignocellulosic fibers: Effect of inherent strength of the particles. *Composites Science and Technology 69*, 1653-1659.

Renner, K., Móczó, J., Suba, P., & Pukánszky, B. (2010b) Micromechanical deformations in PP/lignocellulosic filler composites: Effect of matrix properties. *Composites Science and Technology 70*, 1141-1147.

Renner, K., Móczó, J., Vörös, G., & Pukánszky, B. (2010c) Quantitative determination of interfacial adhesion in composites with strong bonding. *European Polymer Journal 46*, 2000-2004.

Saiah, R., Sreekumar, P. A., Gopalakrishnan, R., Leblanc, N., Gattin, R., & Saiter, J. M. (2009) Fabrication and Characterization of 100% Green Composite: Thermoplastic Based on Wheat Flour Reinforced by Flax Fibers. *Polymer Composites 30*, 1595-1600.

Soykeabkaew, N., Laosat, N., Ngaokla, A., Yodsuwan, N., & Tunkasiri, T. (2012) Reinforcing potential of micro- and nano-sized fibers in the starch-based biocomposites. *Composites Science and Technology 72*, 845-852.

Soykeabkaew, N., Supaphol, P., & Rujiravanit, R. (2004) Preparation and characterization of jute- and flax-reinforced starch-based composite foams. *Carbohydrate Polymers 58*, 53-63.

Sreekala, M. S., Goda, K., & Devi, P. V. (2008) Sorption characteristics of water, oil and diesel in cellulose nanofiber reinforced corn starch resin/ramie fabric composites. *Composite Interfaces 15*, 281-299.

Sreekumar, P. A., Gopalakrishnan, P., Leblanc, N., & Saiter, J. M. (2010a) Effect of glycerol and short sisal fibers on the viscoelastic behavior of wheat flour based thermoplastic. *Composites Part A-Applied Science and Manufacturing 41*, 991-996.

Sreekumar, P. A., Leblanc, N., & Saiter, J. M. (2010b) Characterization of Bulk Agro-Green Composites: Sisal Fiber Reinforced Wheat Flour Thermoplastics. *Polymer Composites 31*, 939-945.

Swanson, C. L., Shogren, R. L., Fanta, G. F., & Imam, S. H. (1993) Starch-plastic materials-Preparation, physical properties, and biodegradability (a review of recent USDA research). *Journal of Environmental Polymer Degradation 1*, 155-166.

Torres, F. G., Arroyo, O. H., & Gomez, C. (2007) Processing and mechanical properties of natural fiber reinforced thermoplastic starch biocomposites. *Journal of Thermoplastic Composite Materials 20*, 207-223.

Turcsányi, B., Pukánszky, B., & Tüdős, F. (1988) Composition Dependence of Tensile Yield Stress in Filled Polymers. *Journal of Materials Science Letters 7*, 160-162.

Wang, G., Thompson, M. R., & Liu, Q. (2012) Controlling the moisture absorption capacity in a fiber-reinforced thermoplastic starch using sodium trimetaphosphate. *Industrial Crops and Products 36*, 299-303.

Wollerdorfer, M., & Bader, H. (1998) Influence of natural fibres on the mechanical properties of biodegradable polymers. *Industrial Crops and Products 8*, 105-112.

Table 1 Particle characteristics of the studied lignocellulosic fibers

Fiber	Abbreviation	D[4,3][a] (μm)	Length[b] (μm)	Diameter[b] (μm)	Aspect ratio[b]
Arbocel CW 630	W35	39.6	93.5	33.3	3.5
Filtracel EFC 1000	W68	213.1	363.4	63.9	6.8
Arbocel FT 400	W126	171.2	235.2	21.8	12.6

a) volume average particle size
b) average values determined from scanning electron micrographs

Table 2 Comparison of Estimated interfacial adhesion in TPS/wood and PP/wood composites

Matrix	Fiber	Coupling	Adhesion, F_a (mJ/m^2)	Parameter B	$B\ln(1/\sigma_0)$
PP	W35	no	150	2.3	-6.8
PP	W35	MAPP	1190	4.7	-13.8
TPS	W35	no	1200	11.6	-21.1
TPS	W68	no	3800	9.4	-17.1
TPS	W126	no	3900	12.6	-22.9

CAPTIONS

Fig. 1 Fiber distribution and the homogeneity of TPS/wood composites studied by microscopy; a) W68, 10 vol%, SEM, b) W126, 10 vol%, SEM, c) W126, 5 vol%, POM, d) TPS, 40 vol%, POM.

Fig. 2 Mechanical properties: a) Effect of wood fiber type and content on the stiffness (a), strength (b) and elongation-at-break (c) of TPS/wood composites; Symbols: (○) W126, (□) W68, (△) W35

Fig. 3 Reinforcement: a) Tensile strength of TPS/wood composites plotted against wood content in the linear representation of **Eq. 1**. Symbols: (○) W126, (□) W68, (△) W35; b) Influence of matrix strength on the reinforcing effect of wood fibers.

Fig. 4 Temperature dependence of the loss modulus of TPS and its wood composites at 30 vol% wood content; decreased mobility in the presence of wood; Symbols: (○) W126, (□) W68, (△) W35

Fig. 5 Acoustic emission testing of TPS/wood composites. a) TPS/W126 composite, wood content: 5 vol%. Symbols: (○) individual acoustic events. Stress (left axis) and cumulative number of events (right axis) vs. elongation traces are plotted as reference. Determination of characteristic stress (σ_{AE}); b) Characteristic stress of the dominating micromechanical deformation mechanism plotted against fiber content; Symbols: (○) W126, (□) W68, (△) W35

Fig. 6 Effect of wood content and fiber type on the equilibrium water absorption (M_∞) of TPS/wood composites. The broken line indicates additivity; Symbols: (○) W126, (□) W68, (△) W35

Fig. 7 Shrinkage of injection molded bars produced from TPS/W68 composites of

various wood contents. Shrinkage was measured 345 days after production.

Fig. 8 Shrinkage of TPS/wood composites: a) Time dependence of the shrinkage of TPS/W126 composites at different wood contents; Symbols: (○) 0, (□) 5, (△) 10 vol%; b) Dependence of equilibrium shrinkage on wood content and fiber type; Symbols (○) W126, (□) W68, (△) W35

Müller, Fig. 1

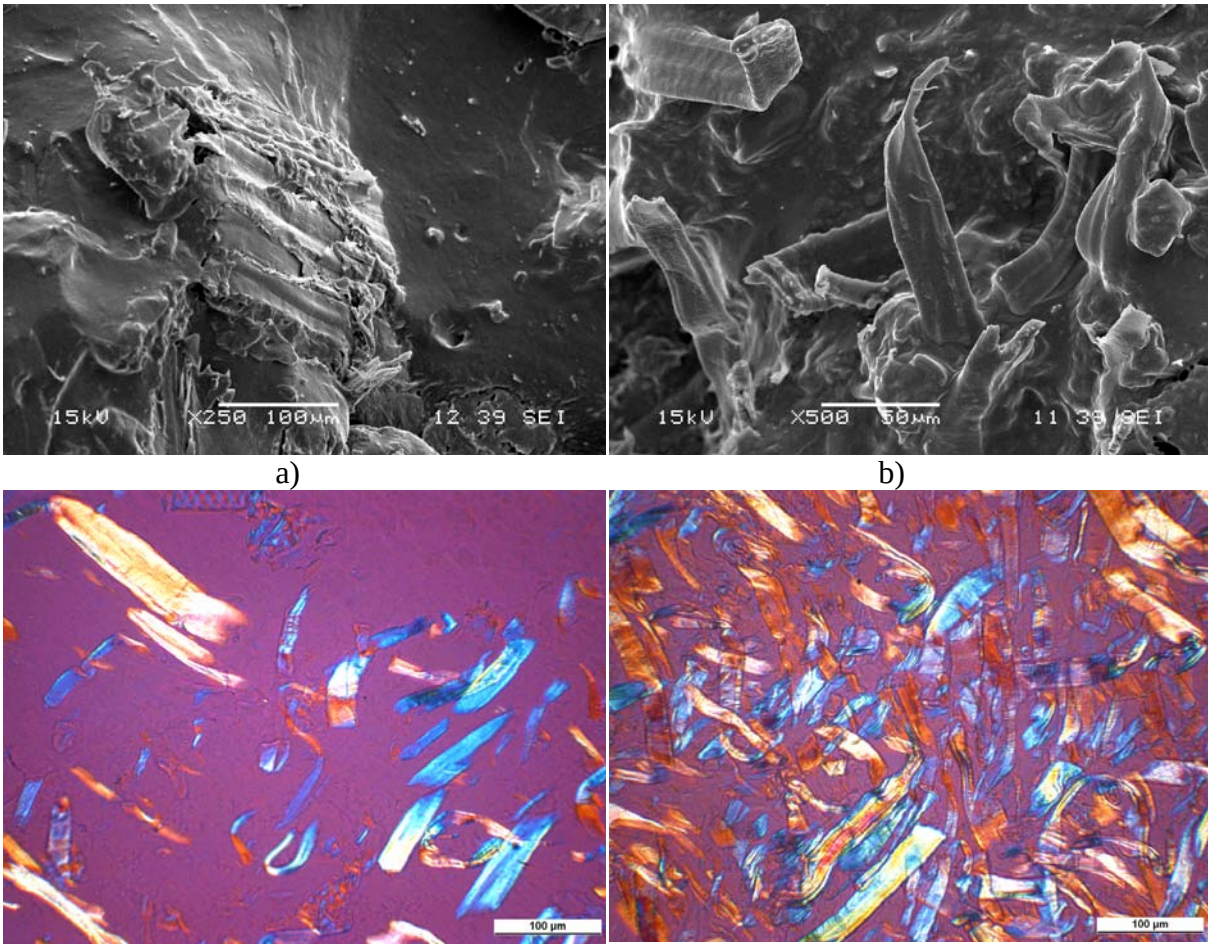

a) b)

c) d)

Fig. 1 Fiber distribution and the homogeneity of TPS/wood composites studied by microscopy; a) W68, 10 vol%, SEM, b) W126, 10 vol%, SEM, c) W126, 5 vol%, POM, d) TPS, 40 vol%, POM.

Müller, Fig. 2

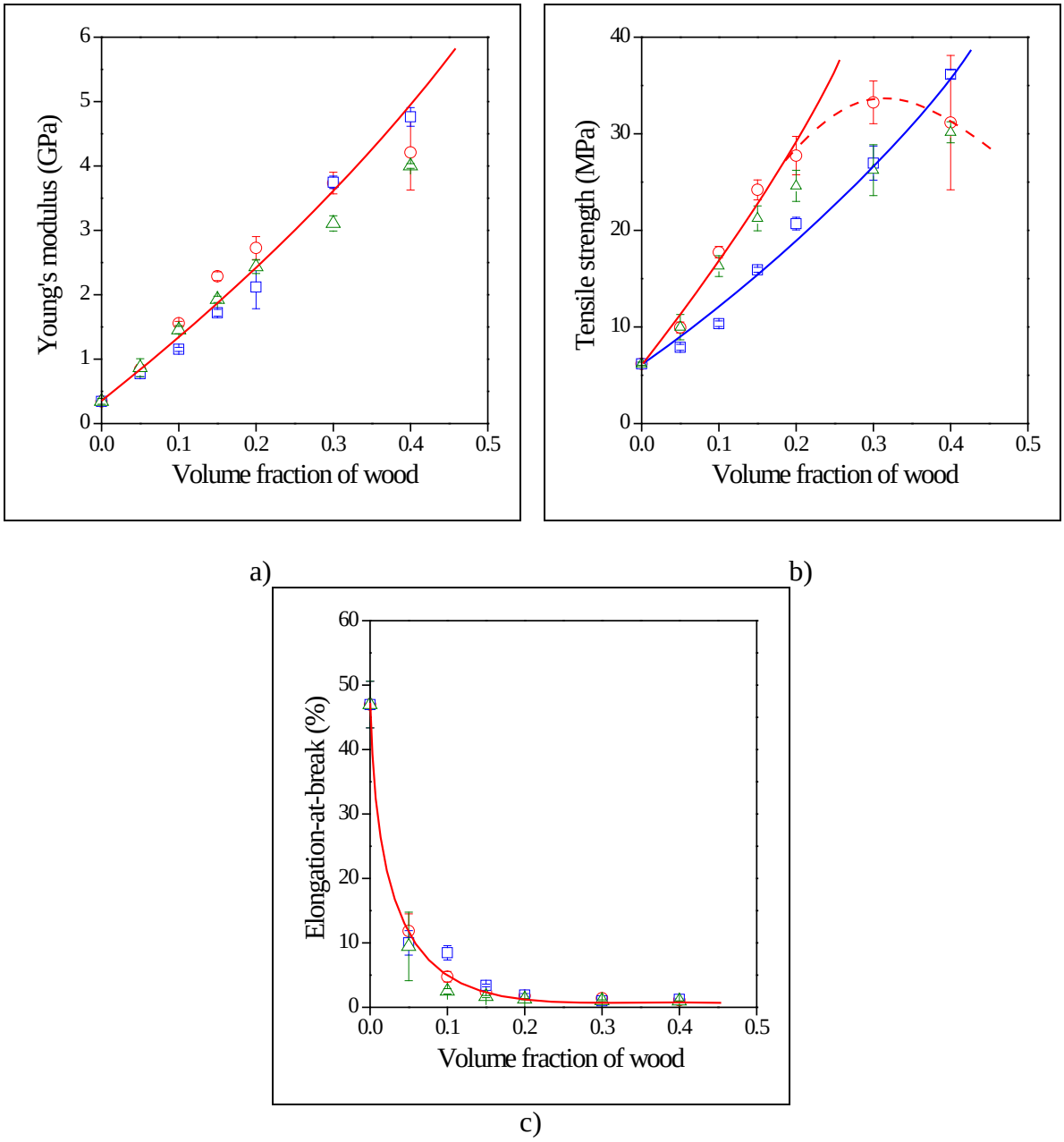

Fig. 2 Mechanical properties: a) Effect of wood fiber type and content on the stiffness (a), strength (b) and elongation-at-break (c) of TPS/wood composites; Symbols: (○) W126, (□) W68, (△) W35

Müller, Fig. 3

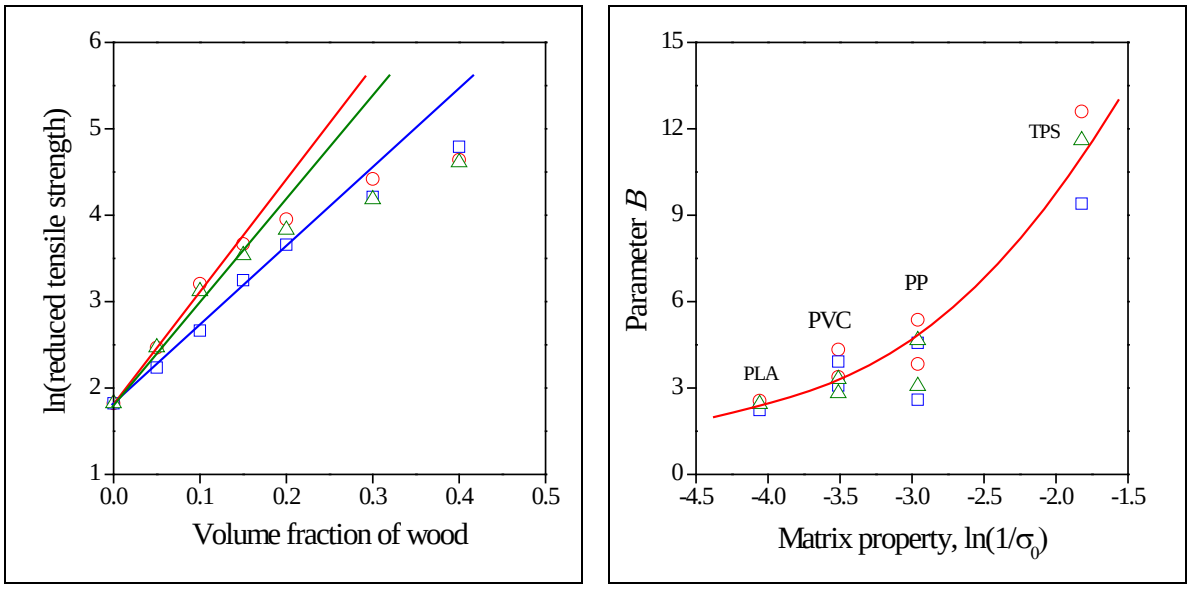

a) b)

Fig. 3 Reinforcement: a) Tensile strength of TPS/wood composites plotted against wood content in the linear representation of **Eq. 1**. Symbols: (○) W126, (□) W68, (△) W35; b) Influence of matrix strength on the reinforcing effect of wood fibers.

Müller, Fig. 4

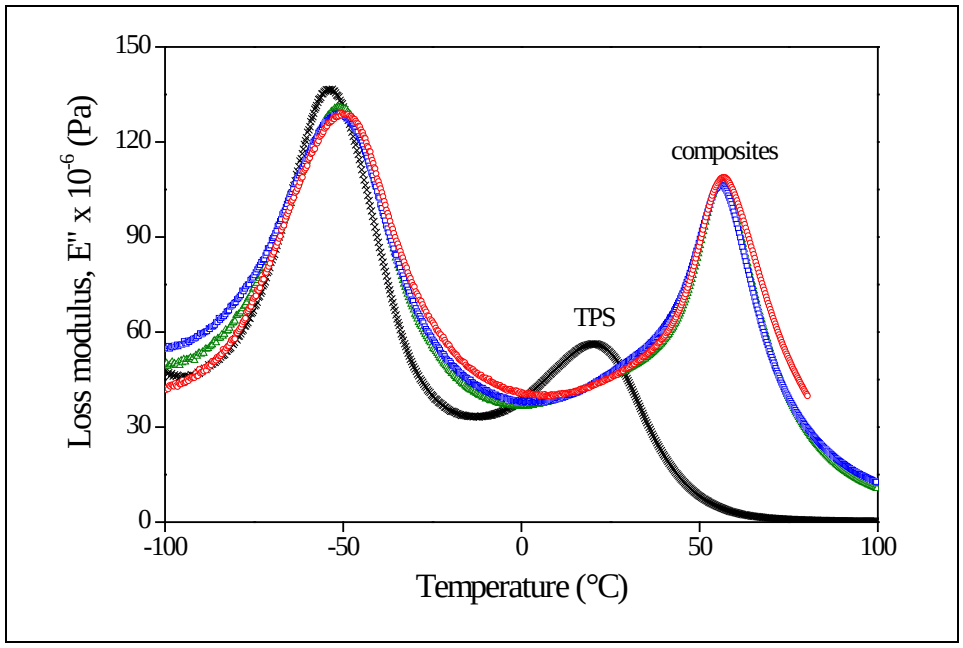

Fig. 4 Temperature dependence of the loss modulus of TPS and its wood composites at 30 vol% wood content; decreased mobility in the presence of wood; Symbols: (○) W126, (□) W68, (△) W35

Müller, Fig. 5

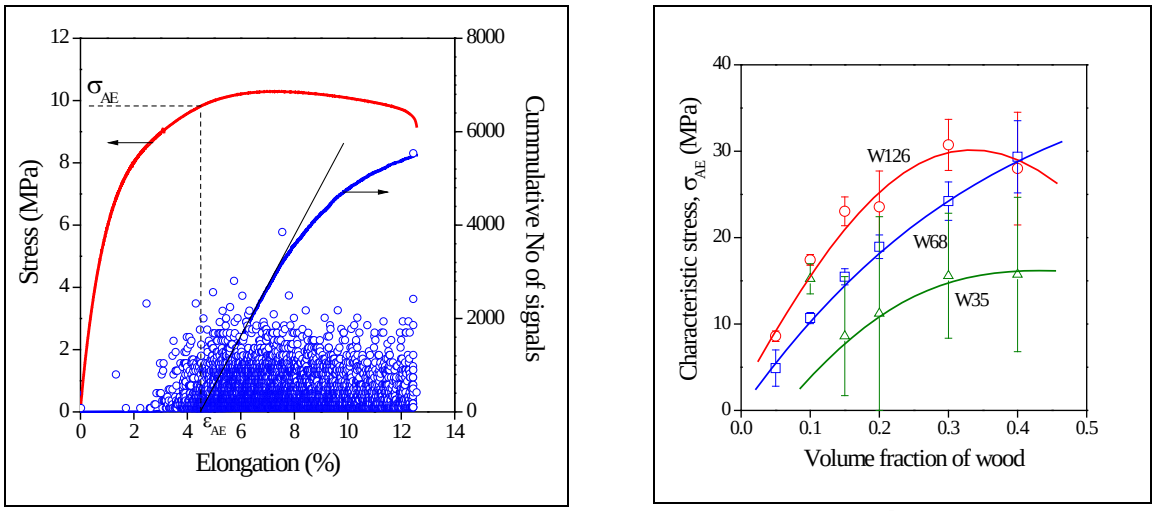

a) b)

Fig. 5 Acoustic emission testing of TPS/wood composites. a) TPS/W126 composite, wood content: 5 vol%. Symbols: (○) individual acoustic events. Stress (left axis) and cumulative number of events (right axis) vs. elongation traces are plotted as reference. Determination of characteristic stress (σ_{AE}); b) Characteristic stress of the dominating micromechanical deformation mechanism plotted against fiber content; Symbols: (○) W126, (□) W68, (△) W35

Müller, Fig. 6

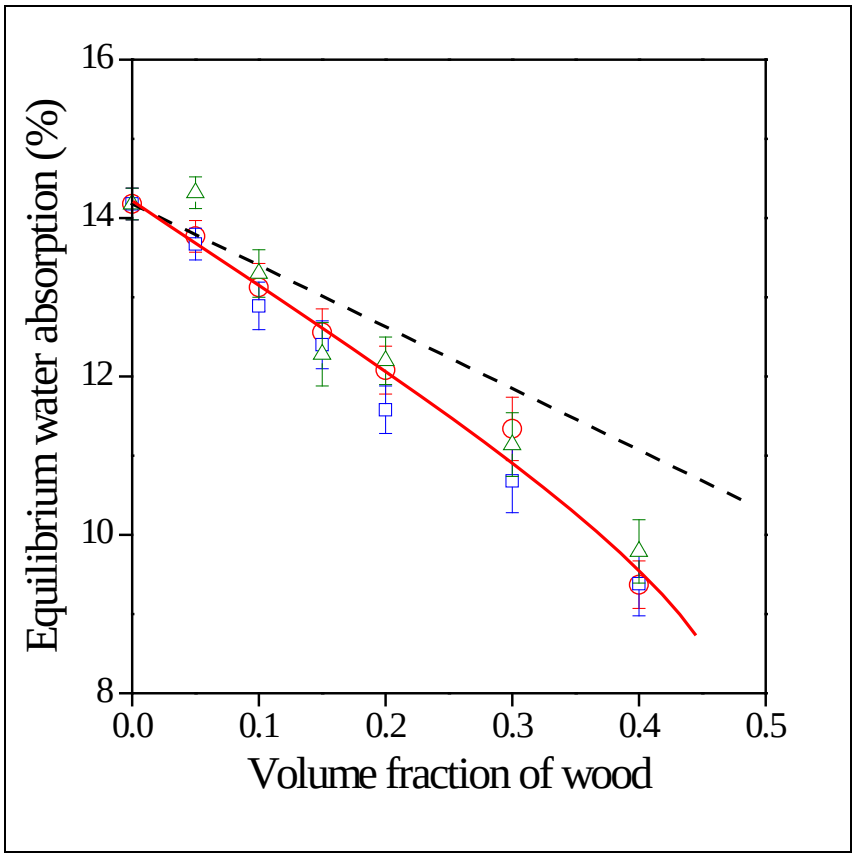

Fig. 6 Effect of wood content and fiber type on the equilibrium water absorption (M_∞) of TPS/wood composites. The broken line indicates additivity; Symbols: (○) W126, (□) W68, (△) W35

Müller, Fig. 7

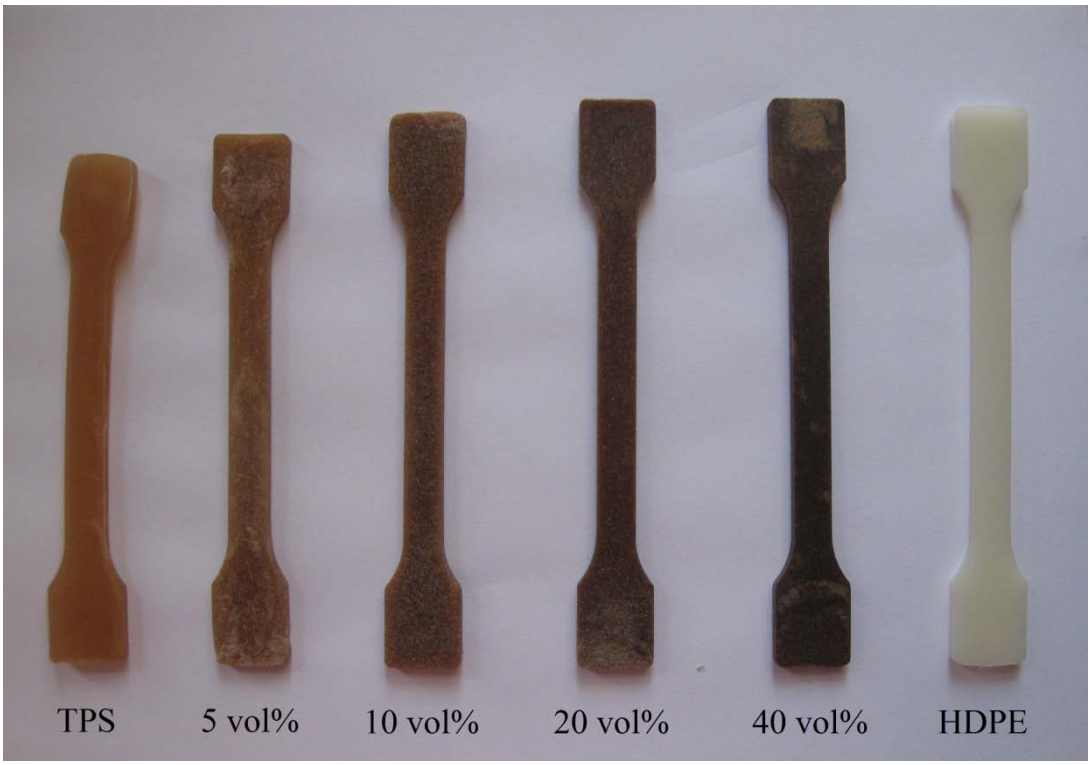

Fig. 7 Shrinkage of injection molded bars produced from TPS/W68 composites of various wood contents. Shrinkage was measured 345 days after production.

Müller, Fig. 8

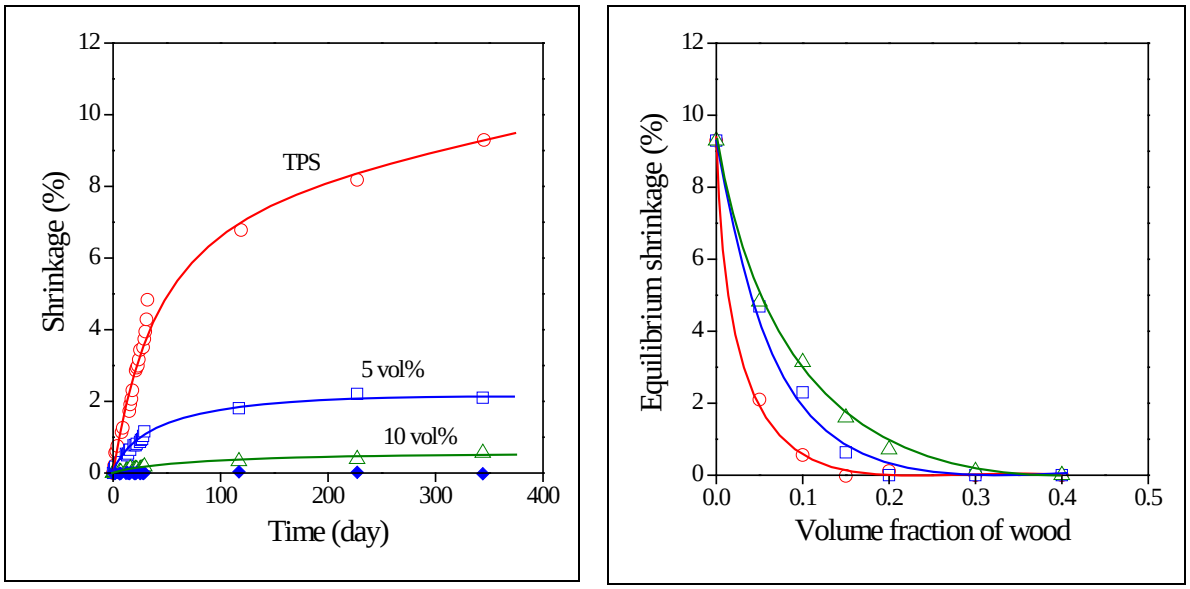

a) b)

Fig. 8 Shrinkage of TPS/wood composites: a) Time dependence of the shrinkage of TPS/W126 composites at different wood contents; Symbols: (○) 0, (□) 5, (△) 10 vol%; b) Dependence of equilibrium shrinkage on wood content and fiber type; Symbols (○) W126, (□) W68, (△) W35